



OPEN Versatile application of fast green FCF as a visible cholangiogram in adult mice to medium-sized mammals

Tomoyuki Niimi^{1,6}, Nanae Miyazaki^{1,6}, Hironobu Oiki^{1,2,6}, Mami Uemura¹, Shihan Zeng^{1,3}, Watcharapon Promsut¹, Noriaki Ota¹, Shunji Nonaka¹, Hajime Takei⁴, Hiroshi Nittono⁴, Seiko Narushima⁵, Ayaka Yanagida¹, Ryuji Hiramatsu¹, Masami Kanai-Azuma³, Shohei Takami^{1,2}, Jun Fujishiro² & Yoshiakira Kanai¹✉

An aqueous solution of a common food dye, Fast Green FCF (FG), mimics cholesteryl-fluorescein to visualize embryonic bile flow via single peritoneal injection into intrauterine mouse embryos. Despite its efficacy in embryos, its suitability for adult mice and small to medium-sized mammals remained uncertain. In this study, we investigated FG cholangiography in adult mice, dogs, and goats. The results demonstrate that FG injection enables progressive cholangiography in these species, highlighting its versatility across different animal models without necessitating specialized equipment. To further evaluate diagnostic utility, FG cholangiography was performed in various mouse models of bile flow disorders. FG successfully visualized dilated lumina in the extrahepatic bile duct of BDL mice and revealed aberrant luminal structures in the gallbladder walls of *Sox17*^{+/-} or *Shh-cre*; *Sox17*^{fllox/-} mice. In *Mab21l1*^{-/-} mice with contracted gallbladders, FG influx was limited to the gallbladder neck. Moreover, stereomicroscopic video analysis of FG influx into the gallbladder post-fasting revealed differences in gallbladder wall state and its bile composition between *Sox17*^{+/-} and wild-type mice, suggesting the potential for detecting variations in gallbladder stored bile properties. These findings underscore the efficacy of FG in facilitating progressive cholangiography across mammalian species.

Keywords Cholangiography, Bile flow, Gallbladder, Mouse, Dog, Goat

Abbreviations

BDL	Common bile duct ligated
FG	Fast green FCF
ICG	Indocyanine green
NIR-II	Second near-infrared region
PBG	Peribiliary gland

Bile is produced in hepatocytes and then transported through the intrahepatic bile ducts to the hepatic and common hepatic ducts for extrahepatic transport. In animals with a gallbladder, bile is transported through the cystic duct to the gallbladder for storage^{1,2}. During the inter-meal period, the bile in the gallbladder is concentrated through its walls, and the concentrated bile is released into the duodenum via the common bile duct by meal stimulation. If this bile flow from the liver to the duodenum is disrupted, biliary atresia occurs, leading to severe hepatic dysfunction and significant morbidity and mortality³.

For the pre- and post-operative evaluation of bile flow in biliary diseases, contrast agents are widely used in medical imaging to enhance the visibility of internal structures or fluids during diagnostic procedures^{4,5}. In humans, gadolinium-based agents are commonly used for MRI, while iodine-based agents are used for X-ray and CT scans for perioperative evaluation of the biliary tree. Since progressive cholangiography is very

¹Department of Veterinary Anatomy, The University of Tokyo, Yayoi 1-1-1, Bunkyo-ku, Tokyo 113-8657, Japan.

²Department of Pediatric Surgery, The University of Tokyo, Bunkyo-ku, Tokyo, Japan. ³Center for Experimental Animals, Tokyo Medical and Dental University, Bunkyo-ku, Tokyo, Japan. ⁴Junshin Clinic Bile Acid Institute, Meguro-ku, Tokyo, Japan. ⁵RIKEN Center for Integrative Medical Sciences, Yokohama, Kanagawa, Japan. ⁶Tomoyuki Niimi, Nanae Miyazaki and Hironobu Oiki contributed equally to this work. ✉email: ykanai@g.ecc.u-tokyo.ac.jp

useful in laparoscopic cholecystectomy to prevent intraoperative bile duct injury⁶, indocyanine green (ICG) has been used as an intravenous cholangiographic contrast medium for human medical practice to localize the site of bile stagnation⁷. After intravenous administration, ICG is taken up by hepatocytes and excreted into the bile duct [Ref.⁸, and references therein]. A near-infrared camera visualized the fluorescence emitted by the ICG in the bile^{9–11}. In mice and rats, cholyl-lysyl fluorescein-labelled bile analogs and NIR-II (second near-infrared region, 1000–1700 nm) fluorescence probes were developed as a tool for the intravital visualization of bile acid transport by using upright two-photon excitation laser scanning microscopy or NIR-II vivo imaging system^{12,13}. In veterinary medicine, choledocholithiasis, biliary sludge, gallbladder mucocele and gallstones are some conditions requiring intraoperative cholangiography⁵. However, these imaging methods have only recently begun at the research level and are not widely used in veterinary medicine, due to the economic aspects including the initial investment in equipment as well as the technical and educational aspects of the veterinary hospital staff.

Existing common food dyes are being used for applications other than traditional food coloring, and their efficacy is being highlighted as they have already been internationally evaluated for safety in animal testing according to common global standards. Recently, tartrazine, a yellow-orange compound 'FD&C Yellow 5' used as a common synthetic pigment in food manufacturing, has been shown to reversibly make engineer skin, muscle, and connective tissue of living rodents to become optically transparent¹⁴. Fast Green FCF (FG), 'FD&C Green No. 3' as a color additive, is also attracting attention as a potential treatment for postoperative cognitive dysfunction by reducing neuroinflammation [15, and references therein]. In our previous study, we newly developed a novel cholangiography method using a food dye FG, which can be administered intraperitoneally through the uterine wall of the mother mouse to visualize the bile flow in the intrauterine mouse embryos¹⁶ (also see Supplementary Movie S1). The contrast agent with blue color can easily visualize the biliary tract of the fetal and perinatal mouse embryos without requiring special equipment. However, it is still unclear whether it is possible to visualize the bile duct and its luminal structure in adult mice and other small- to medium-sized mammals for basic research and veterinary clinical and anatomical practice.

To expand the applicability of FG as a biliary contrast agent, we attempted to visualize the bile duct and biliary system in adult mice, dogs, and goats. Moreover, we comparatively examined FG cholangiography in mouse models of biliary disease, such as common bile duct ligated (BDL) mice, *Sox17* heterozygous mice with gallbladder wall hypoplasia^{16–19}, and *Mab21l1*^{−/−} mice with a contracted gallbladder²⁰. Here, we show that FG contrast agent is a progressive cholangiography for various adult mammals, allowing the detection of the bile duct and its characteristics without requiring special equipment.

Results

Visualization of the extrahepatic bile duct of adult mice, dogs and goats by fast green FCF (FG)

First, wild-type adult mice were used for progressive FG cholangiography. They were placed on a cholecystography table of our own design (Fig. 1B), and the biliary system was observed under a stereomicroscope immediately after FG injection (1 mg/kg bw, iv). As a result, the common hepatic and common bile ducts began to contrast 1–3 minutes after FG injection (Fig. 1B'), and the FG was visible in all extrahepatic ducts, including the gallbladder and cystic duct by 10 min after FG injection (Fig. 1B"). This suggests that the FG can be easily seen even in the extrahepatic ducts of the adult mice under this condition.

Next, we applied the FG cholangiography to the adult dogs (Fig. 1C). Unfortunately, after the first FG administration (0.5 mg/kg bw, iv), FG was only weakly detectable through the fatty tissues surrounding the duct wall in each of the hepatic and common bile ducts in the hilar region. During 10–20 min after the first FG administration, the fatty tissues around the bile duct walls were excised. The FG-labelled bile duct wall served as an indicator and facilitated surgical resection without damaging the bile duct walls (arrowheads in Fig. 1C'). These results suggested that this contrast agent was more suitable for the bile duct walls indicator during bile duct surgery in larger animals, such as dogs, than as a diagnostic contrast agent visible to the naked eye²¹.

Finally, FG cholangiography was performed before the euthanasia of adult goats for dissection training to evaluate its efficacy in preparing observation specimens of the biliary system for dissection. After administration of FG into the external jugular vein of adult goats (10 mg/kg bw, iv), they were euthanized 100 min later and necropsied the next day (Fig. 1D). In FG-treated goats, the extrahepatic bile duct system was clearly visible, whereas in goats not treated with FG, only the gallbladder was visible and the other bile duct systems were difficult to distinguish. These results showed that FG could image the bile duct for approximately 24 h after euthanasia and that it could be easily visualized. This has been shown to be useful in observing the bile duct in anatomy practice.

Progressive FG cholangiography in mouse models of bile duct disease

Next, we comparatively examined FG cholangiography in three mouse models of biliary disease (Fig. 2): (i) common bile duct ligated (BDL) mice, (ii) *Mab21l1*^{−/−} mice with a contracted gallbladder of unknown cause²⁰; Supplementary Fig. S1), and (iii) *Sox17* heterozygous mice (*Sox17*^{+/-} and *Shh-cre*; *Sox17*^{fllox/-} mice, both of which exhibit gallbladder wall hypoplasia^{16–19}).

In the BDL mice, FG cholangiography visualized the dilated lumen of the common bile duct upstream of the ligation site (Fig. 2A). *Mab21l1*^{−/−} mice always show a contracted gallbladder in the normal feeding condition, albeit of proper bile accumulation in the fasted period (Supplementary Fig. S1). FG cholangiography in *Mab21l1*^{−/−} mice (normal feeding) revealed that FG labelled the entire contracted gallbladder in some cases but only the proximal gallbladder region in others, suggesting some difference in the FG influx into the proximal and apical portions of the gallbladder between mutants.

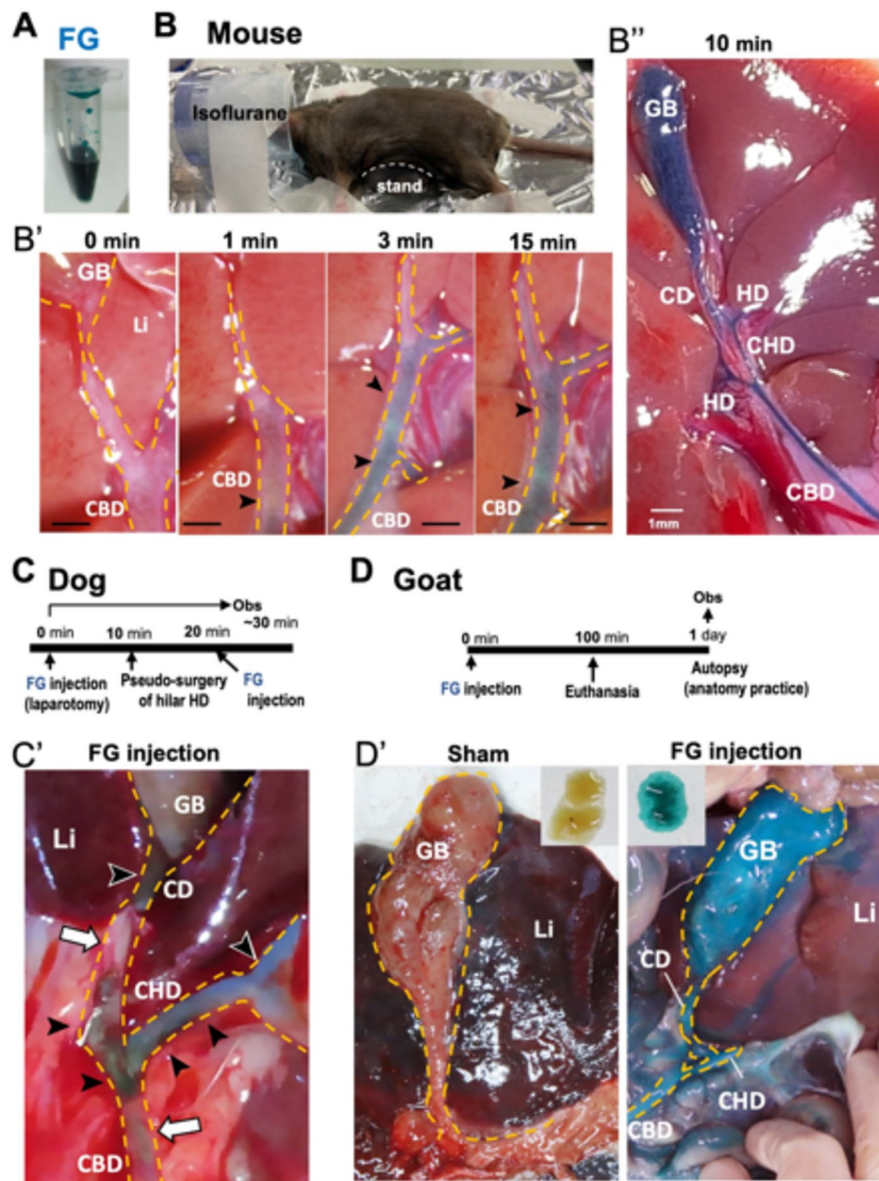


Fig. 1. A novel cholangiography using Fast Green FCF (FG) in adult mice, dogs and goats. **(A)** 1 mg/ml FG solution in 1.5 ml tube. **(B)** Mouse anesthetized with isoflurane is on the original cholecystogram stand (white dotted line) during cholangiography. **(B')** (higher magnified images of bile ducts at hepatic hilus) and **(B'')** (a lower magnified image including the whole gallbladder) show the blue contrast images of the extrahepatic duct at 0, 1, 3, 10 and 15 min after FG administration (1 mg/kg bw). **(C)** In the laparotomy after the first FG injection (0.5 mg/kg bw; iv), the fat and connective tissues covering the extrahepatic bile ducts were removed (pseudo-surgery), and the bile duct images were photographed after additional FG injection (0.5 mg/kg bw at 20 min). Arrowheads indicate the blue contrasted regions visible after removing fat and connective tissue (white arrows, unremoved regions of extrahepatic duct hidden by the fatty tissue around FG-labeled bile duct). **(D)** FG (10 mg/kg bw) was administered via the external jugular vein and euthanized 100 min later. Necropsied the following day at an autopsy practice, Goats were euthanized 100 min after administration of FG (10 mg/kg bw) via the external jugular vein and then necropsied the next day in the dissection practice. In the FG-treated goat, all parts of the extrahepatic bile ducts contrasted in blue are clearly visible. Upper inset, bile in the gallbladder soaked in white paper. CBD common bile duct, GB gallbladder, HD hepatic duct, Li liver. Scale bars: 0.5 mm in **(B')**; 1 mm in **(B'')**.

The *Sox17*^{+/-} and *Shh-cre; Sox17*^{fllox/-} mice show severe gallbladder wall hypoplasia in their *Sox17* gene-dosage-dependent manner¹⁶. However, their gallbladders elongate in a normal direction as the liver grows^{16,22}. FG cholangiography in *Sox17*^{+/-} mice visualized ectopic formation of peribiliary glands (PBGs) in the proximal half of the gallbladder, characteristic of the cystic duct and hepatic ducts^{18,22}. Moreover, FG cholangiography in *Shh-cre; Sox17*^{fllox/-} mice also visualize the narrow lumen of the slender gallbladder with severe gallbladder wall

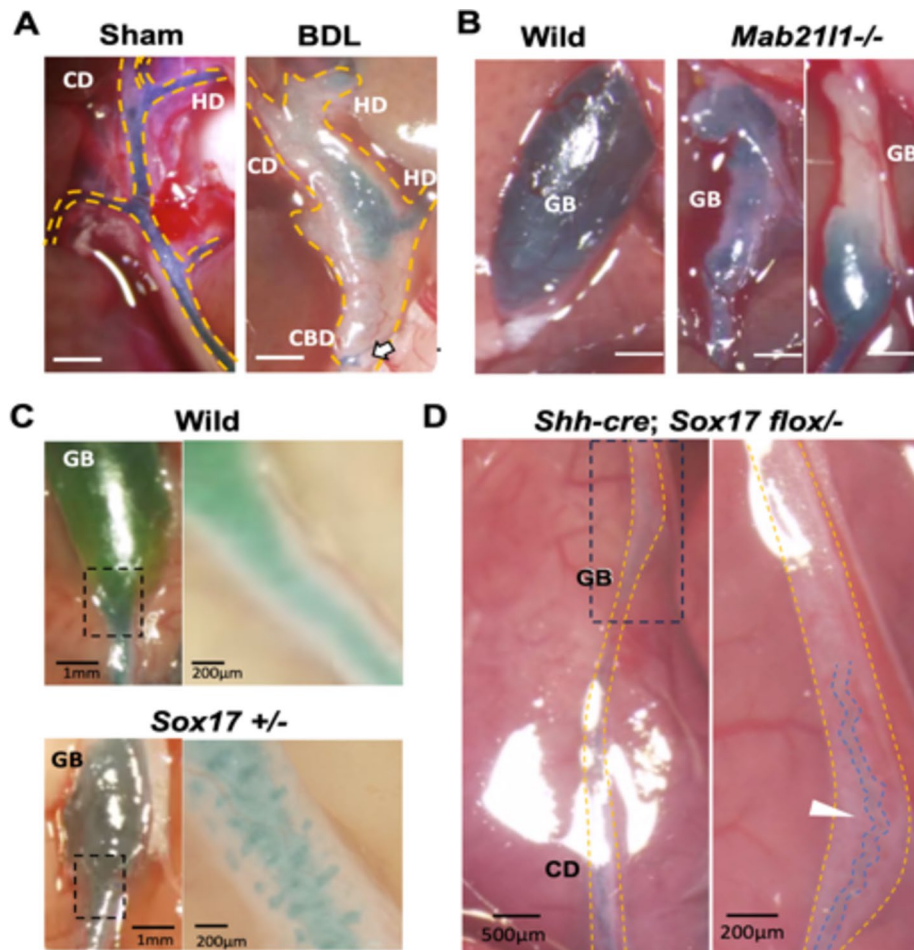


Fig. 2. FG cholangiography in the mouse biliary disease models of bile duct ligation (A), contracted gallbladder (B) and gallbladder wall hypoplasia (C, D). (A) In BDL mice, FG injection visualizes the luminal enlargement of the extrahepatic bile duct (white arrow; common bile duct ligation site). (B) Two *Mab21l1*^{-/-} mice with a spontaneously contracted gallbladder showing the FG-labelled gallbladder in the entire region (left) or only in the proximal region (right). (C) In the *Sox17*^{+/-} mice with hypoplastic gallbladder wall, FG contrast visualizes the ectopically formed peribiliary gland (PBG) in the proximal half of the gallbladder. (D) In the *Shh-cre; Sox17*^{flox/-} mouse with gallbladder wall aplasia, FG contrast visualizes the presence of the long, narrow lumen of the presumptive gallbladder region (white arrowhead; blue dashed line, luminal wall). All mice were fed ad libitum, and images of sham and wild-type controls are also shown. *CBD* common bile duct, *GB* gallbladder, *HD* hepatic duct, *Li* liver. Scale bars: 1 mm in A, B, and the left panel of C; 500 μ m in the left panel of D; 200 μ m in the right panels of (C) and (D).

agenesis (Fig. 2D), suggesting the valuable tool of FG cholangiography to visualize not only the bile duct lumen but also the aberrant internal wall structure of the gallbladder disease models.

Video analysis of FG-labelled bile influx in the gallbladder of wild-type and mutant mice

To clarify the bile influx dynamics into the gallbladder of each genotype of mice, we performed a video analysis of the FG influx within the gallbladder of 12-hour fasted mice (Fig. 3A). The 12-hour fasted condition allows us to correct for the differences in gallbladder constriction between wild-type and mutant mice and to capture the FG-labelled bile flow in the bile-filled gallbladder easily. All mice with wild-type, *Sox17*^{+/-} and *Mab21l1*^{-/-} genotypes demonstrated bile accumulation in the gallbladder after 12-hour fasting (most left plate in Fig. 3B-D), albeit of the slender sac-like gallbladder of the *Sox17*^{+/-} mice¹⁷. In all three genotypes, FG entered the gallbladder toward the apex and filled the entire internal lumen of the gallbladder within 5 min of FG influx (Fig. 3B-D). Even in the wild-type, the time required for FG to label the gallbladder up to the apex varied between individuals. This duration was inconsistent (Fig. 3B). However, the initial influx of freshly FG-labelled bile (blue) formed a well-defined border with the bile stored for 12 h (yellow) in wild-type and *Mab21l1*^{-/-} mice (Fig. 3C). In *Sox17*^{+/-} mice, on the other hand, the border with stored bile in the gallbladder was not well-defined, accompanied by rapid FG diffusion within the gallbladder (Fig. 3D).

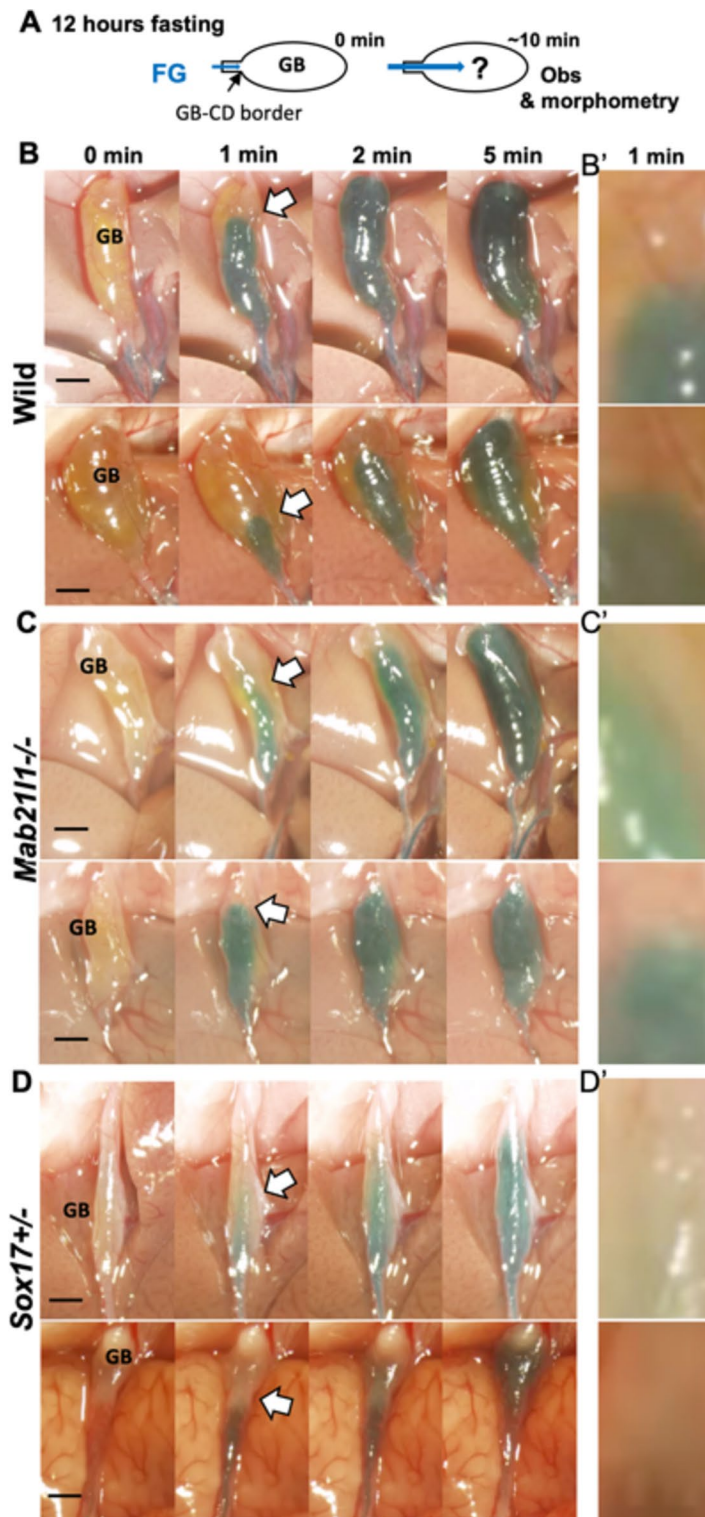
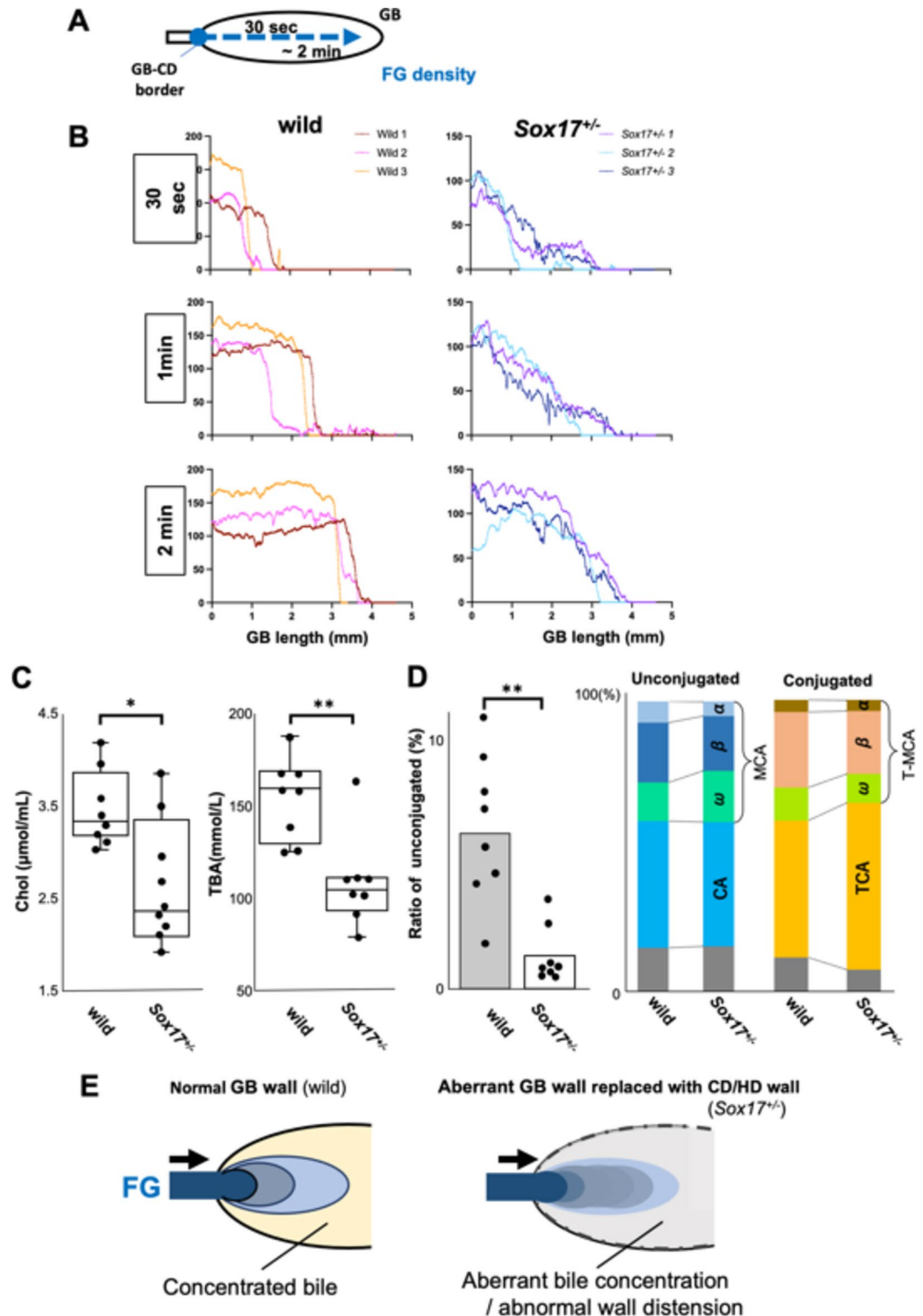


Fig. 3. Video analysis of FG influx and diffusion in the gallbladder of wild-type, *Mab21l1*^{-/-} and *Sox17*^{+/-} mice fasted for 12 h. (A) FG was administered to the mice, fasted for 12 hours, and the kinetics of FG entry into the gallbladder were video recorded under a stereomicroscope. (B–D) Time laps images (0, 1, 2, 5 min) of FG influx in the gallbladders of wild-type (B), *Mab21l1*^{-/-} (C) and *Sox17*^{+/-} (D) mice. Each right inset (i.e., (B'), (C'), (D')) shows a higher magnified view of the border between FG-labelled fresh bile (blue) and fully stored bile (yellow), as indicated by a white arrow (1 min after FG entry in left). The influx of FG-labelled fresh bile causes a two-layer separation with the stored bile in the gallbladder in wild-type and *Mab21l1*^{-/-} mice but not *Sox17*^{+/-} mice. GB gallbladder. Scale bars: 1 mm.



Next, to analyze differences in influx patterns between wild-type and *Sox17*^{+/-} mice, we measured FG density along the axial length of the gallbladder from proximal to distal at 30 s, 1 min, and 2 min after initial FG influx using Image-J (Fig. 4A). In wild-type mice, FG invaded the gallbladder toward the distal end while maintaining a well-defined boundary formed between stored bile and FG (left panels in Fig. 4B). In contrast, in *Sox17*^{+/-} mice, FG density was gradually decreased from the entrance to the distal apex of the gallbladder, following a gradient toward the distal end during the first 2 min after influx (right panels in Fig. 4B). To correct for FG permeability in each gallbladder wall, we estimated the level of relative FG diffusion during the first 30 s at the base of the maximum FG density at 2 min after FG influx into the gallbladder (Supplementary Fig. S2). The initial spread of the relative FG density also formed a well-defined boundary with the stored bile area in the gallbladder of wild-type mice, in contrast to the absence of a boundary between FG and stored bile in the *Sox17*^{+/-} mice (Fig. S2B). The mean diffusion velocity (mm/s) of the FG influx estimated during the first 30 s

◀ **Fig. 4.** Morphometric analysis of FG density and bile acid analysis in the gallbladder of wild-type and *Sox17^{+/-}* mice fasted for 12 h. (A) FG density (blue intensity) along the proximal-distal axis (each of three mice for wild-type and *Sox17^{+/-}* mice) were measured at 0–2 min after FG entry into the gallbladder. (B) Line graphs showing FG dye intensity in the gallbladder of wild-type (three reddish lines on left) and *Sox17^{+/-}* (three bluish lines on right) mice at 30 s, 1 and 2 min after FG influx into the gallbladder (x-axis, the length from the gallbladder-cystic duct border [mm]; y-axis, the absolute value of blue intensity [max value = 255]) (C, D). In (C), box plots show the amount of cholesterol (Chol) (left) and total bile acids (TBA) (right) in gallbladder bile in wild-type and *Sox17^{+/-}* mice fasted for 12 h ($n = 8$ each). In (D), the bar graph shows the average ratio of unconjugated bile acids in TBA and the band graphs show the altered percentage of each bile acid (%) in the amino acid-conjugated (left) or -unconjugated (right) bile acid field between wild-type and *Sox17^{+/-}* mice. * $p < 0.05$; ** $p < 0.01$; p-values were calculated using Welch's t-test. (E) Schematic representation of the different FG dynamics in the gallbladder of wild-type and *Sox17^{+/-}* mice fasted for 12 h. FG influx forms a boundary layer with normally stored bile in the wild-type mice but not in the *Sox17^{+/-}* gallbladder, indicating the abnormal properties of stored bile in *Sox17^{+/-}* mice.

in the gallbladder was significantly higher in the *Sox17^{+/-}* mice than in wild-type mice (wild-type: 2.47 ± 0.31 , *Sox17^{+/-}*: 4.31 ± 2.52 mm/s; $p < 0.05$; $n = 5$ each). These results suggest that FG-enriched fresh bile may readily mix with conventional bile stored in the gallbladder in *Sox17^{+/-}* mice compared to wild-type mice, potentially attributed to the distinctive characteristics of the stored bile.

In addition, we confirmed the distinct FG dynamics in the gallbladder bile prepared from the wild-type and *Sox17^{+/-}* mice fasted for 12 h by using two in vitro systems of a bile drop-on-dish and a bile-filled glass capillary (Supplementary Fig. S3). In both drop and capillary systems, FG was found to move more quickly upward (in the direction opposite to gravity) in the wild-type bile, as compared with the *Sox17^{+/-}* bile (Fig. S3A, B). In the drop-on-dish, FG maintained a clean circular shape on the upper surface of wild-type bile, whereas in the *Sox17^{+/-}* bile, FG randomly diffused as a floating state (Fig. S3A). In the horizontal capillary, FG was found to move upward in the wild-type bile, whereas in the *Sox17^{+/-}* bile, FG diffused in a floating state (Fig. S3B). In the vertical capillary, the FG boundary was more evident in stored bile of wild-type mice as compared with those of *Sox17^{+/-}* mice (Fig. S3C). Such distinct FG dynamics in vitro may reflect the distinct FG influx patterns between wild-type and *Sox17^{+/-}* mice (Fig. 4B).

Bile acid analysis in the gallbladder of wild-type and *Sox17^{+/-}* mice

Since the main effect of the gallbladder wall on bile composition is the removal of water and inorganic electrolytes^{1,2}, we finally measured the gallbladder bile composition in wild-type and *Sox17^{+/-}* mice fasted for 12 h (Fig. 4C, D, Supplementally Table S1). Both cholesterol and total bile acid in gallbladder bile were significantly reduced by about three quarters in *Sox17^{+/-}* mice compared to wild-type mice. The total and individual levels of unconjugated bile acids such as α , β , ω -muricholic acid (MCA) and cholic acid (CA) also showed a significant reduction in *Sox17^{+/-}* mice compared to wild-type mice, resulting in an altered ratio of amino acid-conjugated and unconjugated bile acid composition in their gallbladder fluid between two genotypes (left in Fig. 4D). Interestingly, despite the significant reduction in unconjugated bile acids in *Sox17^{+/-}* mice, each amino acid per total unconjugated bile acid (%) showed a similar composition between wild-type and *Sox17^{+/-}* mice (right in Fig. 4D), suggesting a possible impairment of bile acid enrichment by the gallbladder wall of *Sox17^{+/-}* mice¹⁹.

Discussion

In this study, we concluded that a novel cholangiography method using a common food dye Fast green FCF in adult mice, dogs, and goats yielded several applications (Fig. 1). These applications spanned from detecting the bile duct structures and aberrant gallbladder wall to guiding the extrahepatic bile duct in intraoperative and veterinary anatomy practice. FG administration allowed for visualization of the extrahepatic duct system in adult mice and dogs for approximately 15 min. Moreover, the extrahepatic bile ducts, labelled with FG, remained clearly visible in goats even after one day, making it a valuable tool for dissection practice in veterinary anatomy class. These findings suggest that FG is beneficial as a progressive cholangiographic contrast agent, applicable in both basic researches using mouse models and veterinary practices involving various mammals.

Indocyanine green (ICG) is widely used in medical imaging to enhance the visibility of bile duct structures or fluids during diagnostic procedures for human medical practice⁷. ICG requires a near-infrared camera for contrast, while FG enables contrast the extrahepatic bile ducts with the naked eye. Up to the present time, FG has mainly been used for coloring applications as a food dye. Toxicity tests conducted by the Joint FAO/WHO Expert Committee on Food Additives (JECFA) show no short- or long-term toxicity or carcinogenicity (JECFA Report). It is not carcinogenic in the International Agency for Research on Cancer (IARC) carcinogenic risk assessment (Group 3) (IARC Report), suggesting that FG is a safe food additive in Japan and the USA. ICG is also generally considered to be a safe cholangiographic agent. However, it can cause allergic reactions in rare cases, so the patient's medical history and allergies must be recorded in detail before administration. If FG's safety, including allergy, in intravenous infusion is confirmed, its use in clinical applications during surgery could be considered in the veterinary clinical field. FG is attracting attention as anti-inflammatory and anti-depressive effects to prevent postoperative cognitive dysfunction effects by reducing neuroinflammation, offering both diagnostic and therapeutic potential¹⁵. Moreover, FG is more effective for visualization with the naked eye during surgery in clinical veterinary medicine, where open rather than endoscopic surgery is still common.

FG cholangiography enabled the detection of various biliary abnormalities in mice with biliary system disorders. Initially, in mice with common bile duct ligation, the common hepatic duct (CHD) lumen dilated

upstream of the obstructed site. In the contracted gallbladder of *Mab21l1*^{-/-} mice, bile flow was impeded towards the apex of the shrinking gallbladder (Fig. 2). Moreover, FG administration into the *Sox17* mutants could not only visualize a long and narrow lumen of the severe gallbladder wall agenesis of the *Shh-cre; Sox17*^{+/-} mice, but also ectopically formed PBGs in the aberrant *Sox17*^{+/-} gallbladders walls, a typical pathological character for human biliary atresia¹⁸. Therefore, FG cholangiography can be helpful for macro-anatomical observation/visualization of bile flow in various mouse models.

Interestingly, we observed the formation of a well-defined border of the FG-labelled bile influx into the gallbladder in wild-type mice under a 12-hour fasting condition (Figs. 3B and 4B and E, S2). The bile in the gallbladders is concentrated through water uptake by the biliary epithelium, and the bile acid concentration in the bile sac is about 100–1000 times higher than in the hepatocytes^{1,23}. In contrast to the specific gravity of gallbladder bile, which is about 1.0, the specific gravity of FG is 0.54 (ChemicalBook). Moreover, the specific viscosity of gallbladder bile is higher than that of hepatic bile², together with a positive correlation between mucin and viscosity in gallbladder bile but not in hepatic bile²³. Therefore, the influx of FG-enriched fresh bile may cause a two-layer separation of FG-labelled fresh bile in the gallbladder with fully stored bile, possibly due to the higher density/viscosity of the stored bile after 12 h compared to FG-enriched fresh bile.

On the other hand, during FG influx in *Sox17*^{+/-} mice, fresh FG-labelled bile showed a gradient influx towards the apex without the well-defined border (Figs. 3B and 4B, S2). Moreover, in vitro FG diffusion assay in the drop-on-dish / glass capillary showed a well-defined border formation of FG in the gallbladder bile drop prepared from wild-type, but not from *Sox17*^{+/-} mice (Fig. S3), suggesting a more extensive mixing with conventional bile stored in the gallbladder in *Sox17*^{+/-} mice compared to wild-type mice. The stored gallbladder bile of *Sox17*^{+/-} mice showed a significant dilution of the bile acids together with a considerable reduction of unconjugated bile acids, leading to the possible different characteristics of the stored gallbladder fluid from those of wild-type mice (Fig. 4C–E). The *Sox17*^{+/-} gallbladder, which exhibited hypoplastic walls, was partially replaced by the cystic and hepatic duct-like epithelia, including the PBGs^{18,22}. Since the bile duct walls between the gallbladder and other bile ducts have been shown to be distinctly altered and modulated in bile secretion¹⁸ and involuntary contraction¹⁹, such replacement of non-gallbladder epithelia in the *Sox17*^{+/-} mutants may possibly cause the aberrant characteristics of their stored bile, leading to rapid diffusion of FG-labeled fresh bile without a well-defined border in the gallbladder. Further studies are needed to investigate the mechanisms of such altered bile acid and its fluid dynamics in the gallbladder of *Sox17*^{+/-} mice.

In conclusion, FG, serving as a common food dye, exhibits the remarkable ability to provide progressive biliary contrast in adult mice and across various animal sizes – from small to medium. This versatility suggests its potential for extensive application as a visible contrast agent, eliminating the need for specialized equipment to guide the extrahepatic bile duct in veterinary clinical and anatomy practices. Beyond its current utility for imaging the biliary wall structure, FG may hold promise for the early detection of gallstones, cholecystitis, gallbladder cancer and mucocèles by discerning the nature of the gallbladder wall and its stored bile.

Materials and methods

Animals

Six-week-old male wild-type mice (C57B6J, ICR) were purchased from SLC Japan (Shizuoka, Japan) and bred in the animal room for at least one week before use. The wild-type mice ($n=9$), *Sox17*^{+/-} (i.e., *Sox17*^{+/-}(GFP) and *Sox17*^{+(flox)/-}; $n=5$) and *Shh-cre; Sox17*^{flox/-} mice ($n=5$) mice, a mouse model of biliary atresia^{16–19}, and *Mab21l1*^{-/-} mice with a contracted gallbladder (cause unknown; nine-ten-weeks-old; $n=4$;²⁰) used in this study were obtained by breeding at an animal room of our laboratory. For stereomicroscopic video analysis of FG influx into the gallbladder, all wild-type and mutant mice were fasted 12 h before the experiments to achieve the same level of bile storage in the gallbladder. All mice were maintained on a lighting regime of 12:12 h light: dark with food and water supplied ad libitum unless otherwise stated. Two beagle dogs (six-years-old, 9–10 kg) purchased from Oriental Yeast Co., Ltd. (Tokyo, Japan) were used after another surgical experimental use at laparotomy before being euthanized to donate for dissection. Four Shiba goats, weighing approximately 30 kg, raised at a farm affiliated with the Graduate School of Agricultural and Life Sciences of the University of Tokyo were used. All experiments were performed in accordance with the University of Tokyo Animal Experimentation Regulations. The approval of this study was obtained by the Institutional Animal Care and Use Committee of the Graduate School of Agricultural and Life Sciences, The University of Tokyo (approval numbers: P20-035, P22-018, P21-132, P21-120 and P23-052). The study is reported in accordance with ARRIVE guidelines.

Progressive fast green FCF cholangiography and video analysis of adult mice

Fast Green FCF (FG) (Fig. 1A) was utilized in adult mice, dogs and goats. FG shows maximum biliary output 20 min after administration, and 90.3–92.9% of the bile was excreted within 4 h in rat²⁴ (50% lethal dose of FG is > 2000 mg/kg bw in orally administered rats and > 200 mg/kg bw in orally administered dogs) [¹⁶, and references therein]. In adult mice, intraperitoneal FG administration (30–100 mg/kg bw daily for 12 days before and after surgery) was also shown to improve postoperative cognitive function, rather than causing postoperative sequelae, by using various mouse behavioral tests¹⁵. As for the embryotoxicity, no significant changes in body/liver weight or survival rate just prior to birth were detected in the intrauterine embryos intraperitoneally injected with FG (10 mg/kg; i.p.) at embryonic day 16.5¹⁶.

As for FG cholangiography, the mice with free-fed or 12-hour fasting were used. As for stereomicroscope video analysis, mice were maintained under anesthesia with a 5% concentration of isoflurane. Each mouse was set on a handmade cushion and fixed their limbs with surgical tape on the hot plate (Fig. 1B) under SZX12 stereo microscope (OLYMPUS) equipped with the camera (DP80, OLYMPUS) and imaging software cellSens Standard version 1.16 (<https://www.olympus-lifescience.com/en/software/cellsens/>, OLYMPUS). After laparotomy, the cushion was positioned so the gallbladder, cystic duct, hilar common hepatic, and bile ducts were in the same

plane. The common bile duct ligation was performed at the middle position between the hilar position and the duodenum with nylon thread (7–0) before setting a cushion. After focusing the stereomicroscope onto the gallbladder and hilar hepatic duct, intravenous FG injection through the orbital venous plexus was performed, and the video was immediately recorded using cellSens. The mice were then euthanized by cervical dislocation under deep anesthesia.

Progressive FG cholangiography in adult dogs and goats

After premedication with intravenous administration of atropine (10 mg/kg bw, Nipro ES Pharma, Osaka, Japan) and fentanyl (3 mg/kg bw, Terumo Corporation, Tokyo, Japan), anesthesia of the dogs was induced by intravenous administration of propofol (5 to 10 mg/kg bw to effect, Nichi-Iko, Toyama, Japan), and was maintained by inhalation of isoflurane (DS Pharma Animal Health, Osaka, Japan). The dogs were placed supine on the operating table and the midline incision was made to expose the hilar hepatic duct and common bile duct. After FG injection (0.5 mg/kg bw; i.v. at cephalic vein), the connective tissue covering the outer walls of the cystic duct, hepatic duct, and common bile duct was excised. Approximately 20 min after the first FG injection, FG (0.5 mg/kg bw) was administered again, and FG cholangiography was performed. The dogs were then euthanized by exsanguination under deep anesthesia and donated for veterinary anatomical practice.

The Shiba goats were anesthetized via intravenous injection with isozol (10–15 mg/kg bw, Nichi-Iko Pharmaceutical Co., Ltd., Japan). For administration to the goats, FG (10 mg/kg bw) or saline was injected via the external jugular vein and cervical subcutaneous. The goats were euthanized under anesthesia by exsanguination 100 min after administration. After storage at room temperature overnight, the goats were necropsied.

Morphometric analysis of FG influx in gallbladders in 12-hour fasted mice

The blue intensity of FG was measured using ImageJ²⁵ on videos taken under the stereo microscope. In brief, the images at 30 s, 1 min and 2 min after FG influx were extracted from the videos. Afterwards, only the blue color signals were extracted from the images using Color deconvolution 1.7. The FG density from the cystic duct-gallbladder border (i.e., starting point) to the distal tip of the gallbladder was measured in each video image at three time points by using ImageJ ($n = 5$ in each wild-type or *Sox17*^{+/-} genotype). Moreover, to eliminate permeability differences between sites along the gallbladder wall, we estimated the relative FG density during the first 30 s at the base of the maximum FG density at 2 min after FG influx into the gallbladder. The mean diffusion velocity (mm/s) of the FG influx (> 12.5% of baseline [100%]) was estimated during the first 30 s after the FG entered the gallbladder from the cystic duct.

In addition, to examine FG dynamics in biliary bile more directly, we prepared biliary bile from wild-type or *Sox17*^{+/-} mice fasted for 12 h and then placed 8 μ l drops of bile on the Petri dish. 1 μ l FG (5 mg/ml) was statically added into the bile drop using a glass microinjection pipette ($n = 1$ to 5 mice required for an 8 μ l bile drop; see Fig. S3A). In another FG diffusion assay, the glass capillary (#2-000-010; Drummond Scientific Co., USA) was filled with the bile (1 μ l of each gallbladder) and then placed horizontally/vertically using an adhesive plate (see Fig. S3B, C). 0.3 μ l FG (1 mg/ml) was added to the end of the capillary. In these experiments, FG dynamics in the bile solution were carefully observed under a stereomicroscope from above, together with the naked eye from the side, and in some cases FG density was measured using ImageJ on video recordings.

Bile acid analysis

Gallbladder bile was prepared from the wild-type or *Sox17*^{+/-} mice fasted for 12 h ($n = 8$ for each genotype). The collected bile was frozen and stored at -80 °C. The bile acid analysis was performed according to our previous method using liquid chromatography-mass spectrometry (LS/MS)^{26,27}. In brief, 1 μ l of bile was diluted with 999 μ l of distilled water. 5 μ l of the solution was injected into the LC/MS instrument.

Statistical analysis

All data are shown as mean \pm standard deviation (SD). The diffusion velocity was subjected to a statistical analysis using a Mann-Whitney U test to identify superiority differences using SPSS software. The amount (mmol/L) and ratio (%) of each bile acid were also subjected to statistical analysis using the *Welch's* t-test. A *p*-value ≤ 0.05 was considered indicative of statistical significance.

Data availability

The data presented in this study are available on request from the corresponding author.

Received: 30 July 2024; Accepted: 23 December 2024

Published online: 16 January 2025

References

- Housset, C., Chr tien, Y., Debray, D. & Chignard, N. Functions of the gallbladder. *Compr. Physiol.* **6**, 1549–1577. <https://doi.org/10.1002/cphy.c150050> (2016).
- Luo, X. et al. On the mechanical behavior of the human biliary system. *World J. Gastroenterol.* **13**, 1384–1392. <https://doi.org/10.3748/wjg.v13.i9.1384> (2007).
- Coucke, E. M., Akbar, H., Kahloon, A. & Lopez, P. P. Biliary Obstruction. In: StatPearls [Internet] (StatPearls Publishing, 2022). <https://www.ncbi.nlm.nih.gov/books/NBK539698/>
- Hyodo, T. et al. CT and MR cholangiography: advantages and pitfalls in perioperative evaluation of biliary tree. *Br. J. Radiol.* **85**, 887–996. <https://doi.org/10.1259/bjr/21209407> (2012).
- Larose, P. C. et al. Near-infrared fluorescence cholangiography in dogs: a pilot study. *Vet. Surg.* **53**, 659–670. <https://doi.org/10.1111/vsu.14007> (2023).

6. Saad, N. & Darcy, M. Iatrogenic bile duct injury during laparoscopic cholecystectomy. *Tech. Vasc. Interv. Radiol.* **11**, 102–110. <https://doi.org/10.1053/j.tvir.2008.07.004> (2008).
7. Wu, D. et al. Extrahepatic cholangiography in near-infrared II window with the clinically approved fluorescence agent indocyanine green: a promising imaging technology for intraoperative diagnosis. *Theranostics* **10**, 3636–3651. <https://www.thno.org/v10p3636.htm> (2020).
8. Huang, L. & Vore, M. Multidrug resistance p-glycoprotein 2 is essential for the biliary excretion of indocyanine green. *Drug Metab. Dispos.* **29**, 634–637. <https://dmd.aspetjournals.org/content/29/5/634> (2001).
9. Ishizawa, T., Bandai, Y. & Kokudo, N. Fluorescent cholangiography using indocyanine green for laparoscopic cholecystectomy: an initial experience. *Arch. Surg.* **144**, 381–382. <https://jamanetwork.com/journals/jamasurgery/fullarticle/404783> (2009).
10. Aoki, T. et al. Intraoperative fluorescent imaging using indocyanine green for liver mapping and cholangiography. *J. Hepatobiliary Pancreat. Sci.* **17**, 590–594. <https://doi.org/10.1007/s00534-009-0197-0> (2010).
11. Matsumura, M. et al. Indocyanine green administration a day before surgery may increase bile duct detectability on fluorescence cholangiography during laparoscopic cholecystectomy. *J. Hepatobiliary Pancreat. Sci.* **28**, 202–210. <https://doi.org/10.1002/jhbp.855> (2021).
12. Kamimoto, K., Nakano, Y., Kaneko, K., Miyajima, A. & Itoh, T. Multidimensional imaging of liver injury repair in mice reveals fundamental role of the ductular reaction. *Commun. Biol.* **3**, 289. <https://doi.org/10.1038/s42003-020-1006-1> (2020).
13. Zeng, X. et al. Novel NIR-II fluorescent probes for biliary atresia imaging. *Acta Pharm. Sin. B* **13**, 4578–4590. <https://doi.org/10.1016/j.apsb.2023.07.005> (2023).
14. Ou, Z. et al. Achieving optical transparency in live animals with absorbing molecules. *Science* **285**, 6713. <https://doi.org/10.1126/science.adm6869> (2024).
15. Liu, J. et al. Fast green FCF prevents postoperative cognitive dysfunction via the downregulation of the P2X4 receptor in mice. *Int. Immunopharmacol.* **121**. <https://doi.org/10.1016/j.intimp.2023.110462> (2023).
16. Miyazaki, N. et al. Impact of gallbladder hypoplasia on hilar hepatic ducts in biliary atresia. *Commun. Med.* **4**, 111. <https://doi.org/10.1038/s43856-024-00544-5> (2024).
17. Uemura, M. et al. Sox17 haploinsufficiency results in perinatal biliary atresia and hepatitis in C57BL/6 background mice. *Development* **140**, 639–648. <https://doi.org/10.1242/dev.086702> (2013).
18. Uemura, M. et al. Gallbladder wall abnormality in biliary atresia of mouse Sox17^{+/-} neonates and human infants. *Dis. Model. Mech.* **13**, dmm042119. <https://doi.org/10.1242/dmm.042119> (2020).
19. Higashiyama, H. et al. Embryonic cholecystitis and defective gallbladder contraction in the Sox17-haploinsufficient mouse model of biliary atresia. *Development* **144**, 1906–1917. <https://doi.org/10.1242/dev.147512> (2017).
20. Promsut, W. et al. External genitalia phenotypes of a Mab21l1-null mouse model for cerebellar, ocular, craniofacial, and genital (COFG) syndrome. *Anat. Rec. (Hoboken)* **307**, 1943–1959. <https://doi.org/10.1002/ar.25330> (2024).
21. Hope, W. W. et al. SAGES clinical spotlight review: intraoperative cholangiography. *Surg. Endosc.* **31**, 2007–2016. <https://doi.org/10.1007/s00464-016-5320-0> (2017).
22. Pattarapanawan, M. et al. Anatomical and histological characteristics of the hepatobiliary system in adult Sox17 heterozygote mice. *Anat. Rec. (Hoboken)* **303**, 3096–3107. <https://doi.org/10.1002/ar.24466> (2020).
23. Jüngst, D. et al. Mucin and phospholipids determine viscosity of gallbladder bile in patients with gallstones. *World J. Gastroenterol.* **7**, 203–207. <https://doi.org/10.3748/wjg.v7.i2.203> (2001).
24. Iga, T., Awazu, S. & Nogami, H. Pharmacokinetic study of biliary excretion. II. Comparison of excretion behavior in triphenylmethane dyes. *Chem. Pharm. Bull.* **19**, 273–281 (1971).
25. Rasband, W. S. & ImageJ, U. S. National Institutes of Health, Bethesda, Maryland, USA, <https://imagej.nih.gov/ij/>, 1997–2023.
26. Naritaka, N. et al. Profile of bile acids in fetal gallbladder and meconium using liquid chromatography-tandem mass spectrometry. *Clin. Chim. Acta.* **446**, 76–81. <https://doi.org/10.1016/j.cca.2015.04.008> (2015).
27. Takeda, M. et al. Bile acid profiles in adult patients with biliary atresia who achieve native liver survival after portoenterostomy. *Sci. Rep.* **14**, 2492. <https://doi.org/10.1038/s41598-024-52969-6> (2024).

Acknowledgements

The authors also thank Dr Naoaki Mizuno for the technical advice and support. This study was mainly supported by JSPS KAKENHI (21H00227, 21H02387 and 24H00537) and AMED, Japan Agency for Medical Research and Development (JP21lm0203003j0005).

Author contributions

T.N., N.M.: Writing- original draft, Investigation, Formal analysis, Data curation, Methodology. H.O., M.U., S.Z., W.P., N.O., S.N.: Investigation, Methodology. H.T., H.N., S.N.: Investigation, Data curation, Methodology. A.Y., R.H., M.K.-A.: Writing- original draft, Data curation. S.T., J.F.: Data curation, Funding acquisition. Y.K.: Writing- original draft, Supervision, Conceptualization, Funding acquisition.

Declarations

Competing interests

The authors declare no competing interests.

Additional information

Supplementary Information The online version contains supplementary material available at <https://doi.org/10.1038/s41598-024-84355-7>.

Correspondence and requests for materials should be addressed to Y.K.

Reprints and permissions information is available at www.nature.com/reprints.

Publisher's note Springer Nature remains neutral with regard to jurisdictional claims in published maps and institutional affiliations.

Open Access This article is licensed under a Creative Commons Attribution-NonCommercial-NoDerivatives 4.0 International License, which permits any non-commercial use, sharing, distribution and reproduction in any medium or format, as long as you give appropriate credit to the original author(s) and the source, provide a link to the Creative Commons licence, and indicate if you modified the licensed material. You do not have permission under this licence to share adapted material derived from this article or parts of it. The images or other third party material in this article are included in the article's Creative Commons licence, unless indicated otherwise in a credit line to the material. If material is not included in the article's Creative Commons licence and your intended use is not permitted by statutory regulation or exceeds the permitted use, you will need to obtain permission directly from the copyright holder. To view a copy of this licence, visit <http://creativecommons.org/licenses/by-nc-nd/4.0/>.

© The Author(s) 2025